의학석사 학위논문

Role of Fibroblast Growth Factor 13 in fatty acid induced insulin resistance in skeletal muscle

FGF13 이 지방산에 의한 골격근 인슐린 저항성에 미치는 영향

2015 년 **8** 월

서울대학교 대학원

분자의학 및 바이오제약 학과

조 윤 경

Abstract

Fibroblast growth factors (FGFs) are categorized as paracrine, endocrine and intracrine and are involved in development, cell proliferation, differentiation and metabolism. The secreted FGFs function by interacting with FGF receptors while intracellular non-secreting FGFs interact with voltage gated sodium channels. FGF13 is a member of the intracellular fibroblast growth factor family. FGF13 has various transcript variants by alternatively splicing at 5' end. This study was aimed to investigate the regulation of FGF13 in diet induced obese mice and in fatty acid induced insulin resistance in skeletal muscle. FGF13 isoform 1 was mainly distributed in brain and adipose tissues while FGF13 isoform 2 was predominantly expressed in heart and muscle. I have demonstrated that both muscle and adipose expression of FGF13 was reduced in 12 week high fat fed mice. 24 hour exposure to palmitate decreased FGF13 isoform 2 in C2C12 muscle cells. I also found that palmitate decreased FGF13 through TLR4 pathway. Moreover, when FGF13 was knockdown, immediate early genes of downstream ERK/JNK was suppressed. To further investigate the role of FGF13 in insulin signaling model, FGF13 was overexpressed or knocked down on C2C12 myotubes. I was able to confirm that overexpressing FGF13 could recover AKT signaling during palmitate

treatment while knockdown reduced phospho-AKT. Moreover, overexpression of FGF13 reduced phospho-JNK which is known to affect insulin signaling. These findings suggests that FGF13 protein have a role in insulin signaling pathway in fatty acid induced insulin resistance.

Key words: Fibroblast Growth Factor 13, Fibroblast Growth Factor Homologous Factor 2, insulin resistance, saturated fatty acid, palmitate, type 2 diabetes, obesity, MAPK

Student Number: 2013-24045

Contents

List of Figures

List of Tables

Introduction

Fibroblast growth factors (FGFs) are a family of structurally related polypeptide that are encoded by 22 genes sharing 13-71% sequence identity [2]. FGFs have various roles in cell proliferation, migration and differentiation and involved in developmental, neurological and metabolic disease [1, 2]. FGFs are classified as intracrine, paracrine and endocrine family. One of the most well-known endocrine FGF is FGF21. FGF21 is an emerging potential treatment of diabetes mellitus as it plays an important role in metabolic pathway. FGF21 have beneficial effects on glucose and lipid metabolism, insulin sensitivity and fat utilization [3]. The other molecule of interest, and the focus of this article, is FGF13. FGF13 is a member of the intracrine FGF and it is known as the ancestral gene of the FGF family in evolution [1]. Because FGF13 has substantial sequence similarity to FGFs, it is also referred to as fibroblast growth factor homologous factor 2 (FHF2) [5]. These FGF homologous factors' only known interactions are with voltage-gated sodium channels and MAPK scaffold protein islet brain 2 (IB2) [6]. This non-secretory protein FGF13 lack cleavable secreted signal sequence and cannot bind with FGF receptor tyrosine kinases [7]. FGF13 has been widely studied in neurological field as it is a candidate gene for X-chromosome-linked mental retardation (XLMR) [8] and FGF13 plays role in stabilizing microtubules and regulate neuronal polarization [9]. However,

currently no studies have been reported on FGF13 in metabolic pathway. FGF13 attract attention as microarray analysis from recent study demonstrated that both FGF21 and FGF13 are up-regulated by peroxisome proliferator-activated receptor γ (PPARγ) agonists and in adipose tissue of diabetic mice [4].

Type 2 diabetes is a metabolic disorder that results from decreased insulin secretion in pancreas and insulin resistance in muscle, liver and adipose tissues [10]. High caloric intake and reduced energy expenditure culminate in obesity which leads to insulin resistance and type 2 diabetes mellitus. Enlarged adipose tissue in obesity releases excess amount of free fatty acids and inflammatory mediators such as tumor necrosis factor-α (TNFα) into circulation [11]. Free fatty acids is a major link between obesity and type 2 diabetes which cause insulin resistance in peripheral tissues. Acutely raising plasma free fatty acids levels activates, c-Jun NH2-terminal kinase (JNK) via toll like receptor 4 (TLR4) [12]. When JNK is activated, it disrupts insulin signaling by decreasing tyrosine phosphorylation of insulin receptor 1 or 2 (IRS1/2) [13]. This mechanism inhibits activity of the IRS/PI3K/AKT pathway which is the major pathway of insulin actions controlling glucose uptake, glycogen synthesis and lipolysis [14].

This research was initiated by the evidence of increased mRNA expression of FGF13 by PPARγ agonists in adipose tissue and its interaction

with MAPK scaffolding protein. These clues lead me to question whether FGF13 may play role in metabolic pathway. Therefore, in this study, I examined the expression of FGF13 in adipose tissue and skeletal muscle in diet induced obesity (DIO) mice model and the regulatory mechanism of FGF13 expression in skeletal muscle cells. Then, the effect of FGF13 on insulin signaling in C2C12 myotubes was investigated using FGF13 knockdown or overexpression.

Materials and Methods

Animal Care and Experiments

Mice were housed 5 per cage in specific pathogen free (SPF) facility in Biomedical Center for Animal Resource and Development (Seoul National University, Korea), with a 12 hour light cycle at 22-24 Cº. All mice had access to food and water ad libitum and body weight was recorded every week. The control group- 5 week old C57BL/6 (B6)- was fed with standard rodent chow (Cargil Agri Purina, Gangnam-gu, Seoul, Korea) while diet induced obesity group (DIO) was fed with 58 Kcal% fat with sucrose Surwit Diet (D12331, Research Diets Inc., New Brunswick, NJ) for 12 weeks and sacrificed.

For genetic diabetic mice model comparisons, 5 week old C57BLKS/J-*db/db* (*db/db*) and lean controls (*db/m*) mice were purchased from SLC (SLC, Shizuoka, Japan). Tissues were obtained at 13 weeks of age. For tissue analysis, mice were anesthetized with zoletil (50mg/kg); tissues were isolated and snap-frozen in liquid nitrogen. All animal studies were approved from Biomedical Center for Animal Resource and Development, Seoul National University.

Cell Culture and differentiation

Mouse C2C12 myoblasts were maintained in Dulbecco's Modified Eagle Medium (DMEM) supplemented with 10 % fetal bovine serum (Invitrogen, Carlesbad, CA), 5 g/ml. When cells are 80% confluent, differentiation was induced by switching the medium to 2 % horse serum which was changed to fresh medium every other day. 4 days after 2 % horse serum addition, differentiated C2C12 myotubes were incubated in 2 % horse serum containing 1.5 % bovine serum albumin (BSA) in either presence or absence of palmitate. After 24 hour incubation, cells were harvested for RNA and protein preparation.

Small interfering RNA treatment

50 nM or 100 nM FGF13 siRNA (Dharmacon, Chicago, Il) or 50nM of TL4 siRNA (Dharmacon) (1-CAA ACU AUA CAG CCG ACA A; 2-ACU UGU ACA CCU CGG AAC A; 3-CAA GAC CAG CUG CGA CAA A; 4-GGC AAU GAA CAG CGA GGG A) was incubated with RNA iMAX (Invitrogen) in 100ul of serum-free DMEM for 20 minutes. Mixture was treated to the cells with addition of 400ul of serum-free DMEM for 5 hours and the media was changed back to 2 % horse serum.

Generation of adenovirus-FGF13

Expression vectors containing isoform 2 domain of mouse FGF13 were constructed by subcloning the corresponding cDNA from mouse gastrocnemius muscle. Then it was ligated into pcDNA3.1/His A using KpnI and XhoI sites. Adenoviruses encoding mouse FGF13 were generated by insertion of ORF into pAdTrack-CMV. GFP expressing adenoviruses (Ad-GFP) were constructed as described previously.

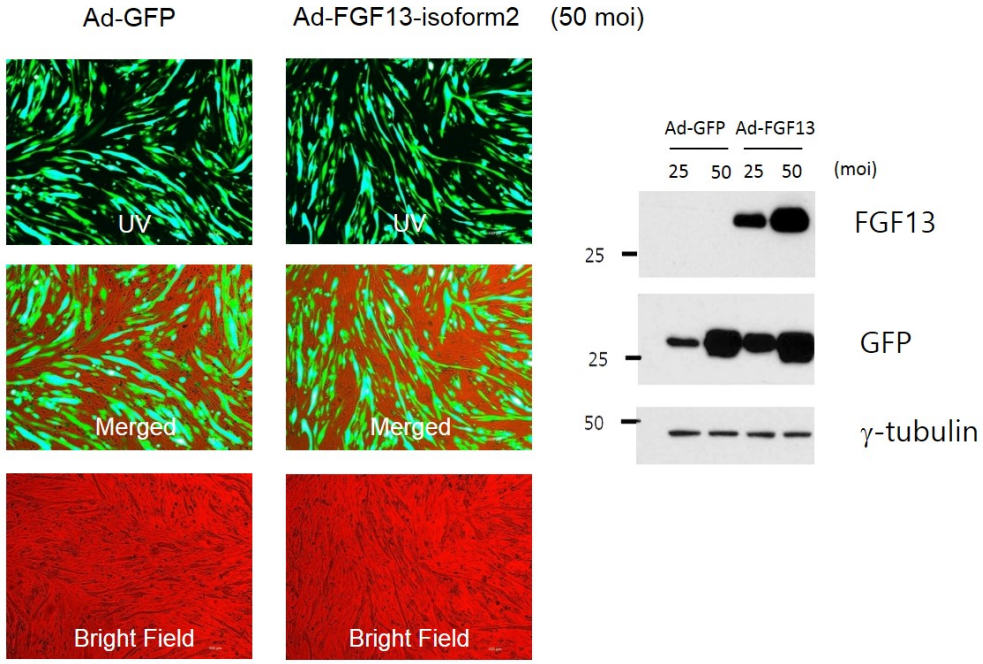

Figure 1. Generation and expression of adenovirus-FGF13 isoform 2

Western blot analysis

Cells were harvested in lysis buffer containing 20 mM Tris-HCl (pH 7.4), 5 mM $Na_4P_2O_7$, 100 nM NAF, 2 mM Na_3VO_4, and 1% NP-40 buffer in addition of protease inhibitors (1 µg/µl aprotinin, 1 µg/ul leupeptin, and 1 mM PMSF (Sigma, St.Louis, MI). Centrifugation was done to remove cell debris for 20 minutes at 4 Cº. Protein quantification was done by using Bicinchoninic-acid (BCA) assay. 30 µg of proteins were loaded in SDS-polyacrylamide gel then transferred onto nitrocellulose membrane (Whatman, Germany).

For mice tissues, snap frozen tissues were minced and was incubated in lysis buffer on the rotator for 2 hours at 4 C°. Antibodies against gamma-tubulin (Sigma-Aldrich, St. Louis, MO), FGF13 (Abcam, Cambridge, UK) were used. Antibodies against insulin receptor substrate-1 (IRS) and phospho-IRS-1 was purchased from Santa Cruz Biotech (Santa Cruz, CA). Antibodies against AKT, phospho-AKT, ERK, phospho-ERK, JNK and phospho-JNK were purchased from Cell Signaling Technology (Danvers, MA).

RNA isolation, Reverse Transcriptase-PCR and quantitative PCR analysis

Trizol reagent (Invitrogen) was used to extract total RNAs of differentiated C2C12 cells according to the manufacturer's instructions. cDNAs were synthesized by 1μg of total RNA, 5 μl of 5X first-strand buffer, 2.5 μl of 100 mM DTT, 1 μl of Oligo (dT), 1.25 μl of 10 mM dNTP Mix, 0.25 μl of RNase inhibitor, 1μl of RTase (Invitrogen) and RNase free water up to 25 μl. The mixture was incubated at 37 °C for 1 hour and the reaction was inactivated by heating at 70 °C for 10 minutes. Then each cDNA was used as a template for amplification in PCR with their specific primers (Table 1). The PCR products were analyzed by electrophoresis on 1.5 % agarose gel. Moreover, quantitative real-time PCR was performed to analyze RNA expression levels of genes by using SYBR-master mix (Takara, Otsu, Shiga, Japan) and AB 7500 Real-time PCR system (Applied biosystems, CA). The primers for qPCR are listed on table 2.

Statistical Analysis

Statistical analysis of data was done with GraphPad Prism version 5.0 (GraphPad Software, Inc., La Jolla, CA). Unpaired t-test (with 95 % C.I.) and one-way analysis of variants (ANOVA) was used to measure the differences between means. Data were expressed as a mean ± standard error, and data with p-value less than 0.05 are denoted as statistically significant.

Table 1. Mouse FGF13 mRNA splice variants examined in this study Primer Sequences used for RT-PCR (Corresponding to Fig 3 and 7)		
Target	Primer Sequences (5'→3')	Product Size (bp)
FGF13 isoform1	Forward 5'-ATGGCGGCGGCTATCGCCAG-3' Reverse 5'-ATGGATTTGCCTCCATTCAG-3'	716bp
FGF13 isoform2	Forward 5'-AATGCCTGCAAGTGTGTCAG-3' Reverse 5'-CACTTCCAGATCGGGAGAAC-3'	594bp
FGF13 isoform3	Forward 5'-ATGGCTTTGTTAAGGAAGTCATATTC-3' Reverse 5'-ATGGATTTGCCTCCATTCAG-3'	557bp
*The NCBI page at the link below was consulted. It listed three variants of the mouse FGF13 transcript, encoding three isoforms of FGF13 polypeptide. Expression of isoforms 1/2/3/ were detected using a Oligo(dT) primer. http://www.ncbi.nlm.nih.gov/gene/14168		

Table 2 Primer Sequences used for quantitative PCR (species: *mus musculus*)	
Target	Primer Sequences (5'→3')
FGF13 (all variants)	Forward 5'- CCTCGGAACATTTCACACCT -3' Reverse 5'- AGTGGTTTGGGCAGAAAATG -3'
FGF13 isoform1	Forward 5'- CTTTTCCCGGGTCAAACTCT -3' Reverse 5'- ACCAAAGACGAGGACAGCAC -3'
FGF13 isoform2	Forward 5'- CCCCTTTCGTGCTAAGTGTC -3' Reverse 5'- CTGCAGTTGCAAGTGGTAGC -3'
C-Fos	Forward 5'-TTGAGCGATCATCCCGGTC-3' Reverse 5'-GCGTGAGTCCATACTGGCAAG-3'
EgrI	Forward 5'-TCGGCTCCTTTCCTCACTCA-3' Reverse 5'-CTCATAGGGTTGTTCGCTCGG-3'
C-Jun	Forward 5'-GTCCTCCATAAATGCCTGTTCC-3' Reverse 5'-GATGCAACCCACTGACCAGA -3'
PGC1a	Forward 5'- ACCTGACACAACGCGGACAG-3' Reverse 5'- TCTCAAGAGCAGCGAAAGCG-3'
GLUT4	Forward 5'-AGCTGTGCTTGGCTCCCTTC-3' Reverse 5'-CTTGTGGGATGGAATCCGGT-3'
GAPDH	Forward 5'- AGGTCGGTGTGAACGGATTTG-3' Reverse 5'- TGTAGACCATGTAGTTGAGGTCA-3'

Results

I. Expression profile of FGF13 in mouse tissues

The structure and expression of FGF13 isoform mouse tissues

I report here the characterization of isoforms of FGF13-isoform 1, 2 and 3 which are generated by alternatively splicing. Isoforms of FGF13 mainly vary from the 5'UTR sequence but they share four of the same exons before 3'UTR (Fig. 2). Expression of alternative splice variants of FGF13 are regulated in tissue-specific manner. Isoform 1 is mainly expressed in whole brain tissue and adipose tissues such as epididymal adipose tissue (EAT), brown adipose tissue (BAT) and visceral adipose tissue (VAT). On the other hand, expression of FGF13 isoform 2 was mainly expressed in heart, and skeletal muscle. FGF13 isoform 3 was mainly present in adipose tissues (Fig. 3).

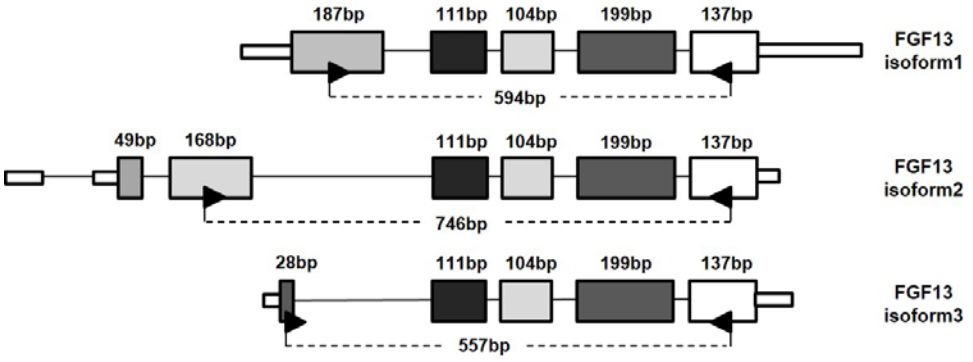

Figure 2. Structures of alternatively spliced FGF13 transcript variants- isoform 1, 2 and 3*

Each box represents an exon. Intron lengths are not drawn into scale. The 5' UTR is shown to the right and 3' UTR is on the left. These transcripts were identified from cDNA of mouse tissue.

'▶'represents forward primer site and '◀'represents reverse primer site of each FGF13 isoforms.

*The NCBI page at the link below was referred. Out of eight listed variants of mouse FGF13 transcript, a, b, and d variant- corresponding to isoform 2, 1, and 3, was studied in this report.
[http://www.ncbi.nlm.nih.gov/IEB/Research/Acembly/av.cgi?db=mouse&term=fgf13&submit=Go]

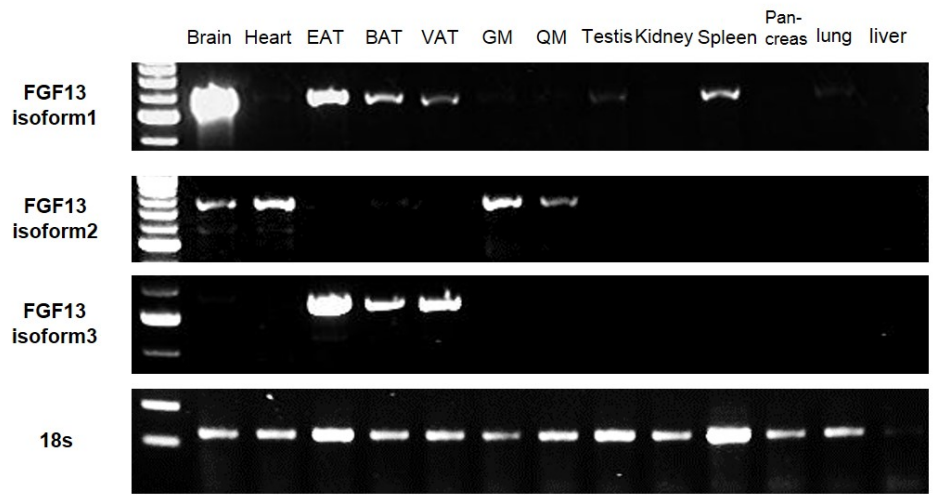

Figure 3. Expression of FGF13 isoform 1, 2 and 3 in various adult mouse tissues.

mRNA of mouse tissue was subjected to RT-PCR for 25 cycles for expression of FGF13. Primers of FGF13-isoform 1, 2 and 3 were designed to uniquely detect each isoform. The housekeeping gene 18s was amplified for 15 cycles.

II. Expression of FGF13 in metabolic tissues in diet induced obesity

Expression of FGF13 in adipose tissue and skeletal muscle in mouse models of obesity

B6 mice were fed with 60 % sucrose high fat diet for 12 weeks and their adipose tissues and gastrocnemius muscle tissues were subjected to RNA and protein extraction. The diet induced obesity (DIO) group weighed about 47 g in average while control diet group weighed 29 g at 12 weeks of high fat diet (Fig. 4A). In the DIO mouse, mRNA expression of FGF13 was decreased by 52 % in white adipose tissue as compared with control diet; similar trends were observed in skeletal muscle tissue showing reduction of FGF13 expression by 40% (Fig. 4B and 4C). Moreover, to compare expression levels of FGF13, IRS and AKT in DIO model, white adipose tissues were collected for western blot analysis (Fig 5A). Interestingly, in DIO mouse tissue, protein levels of IRS and AKT were decreased and FGF13 expression was also noticeably decreased as well (Fig 5B).

I then assessed whether db/db mice show same expression pattern of FGF13 in adipose tissue and muscle tissue. However, the protein level of FGF13 was upregulated in adipose tissue of db/db mice compared to the control db/m mice (Fig. 6).

Expression of FGF13 in various types of cells

To observe which cells lines FGF13 is mostly expressed in, RNAs of different cell lines: 3T3L1 (adipocyte), RAW 264.7 (macrophage), C2C12 (myotubes), NIT-1 (β-cell), MIN6 (β-cell) and islet was extracted. RNA of FGF13 isoform 1 and 2 was only detected on fully differentiated C2C12 and macrophage cell (Fig. 7).

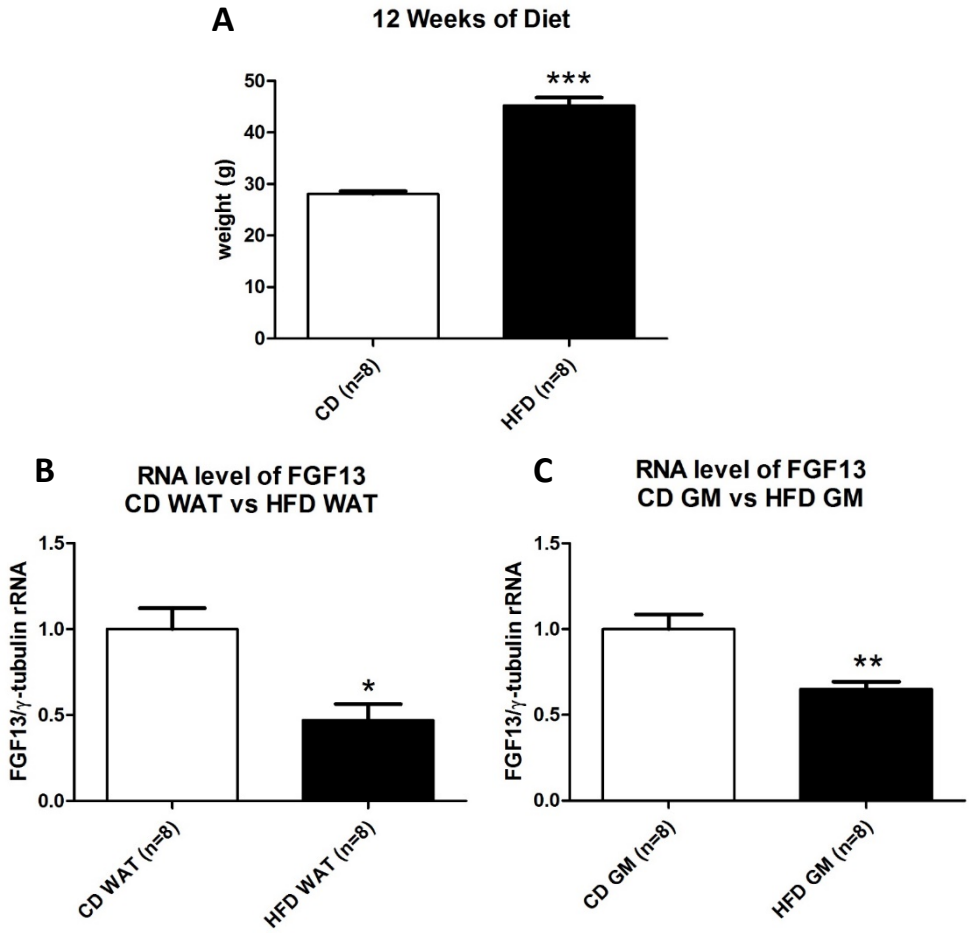

Figure 4. mRNA level of FGF13 in white adipose tissue and gastrocnemius muscle in diet induced obese mouse model

(A) High fat diet fed B6 mice successfully gained more weight than control diet group. (B, C) Expression of FGF13 mRNA is decreased in white adipose tissues and gastrocnemius muscle by half fold. (*p<0.05, **P<0.005, ***p<0.001 vs CD)

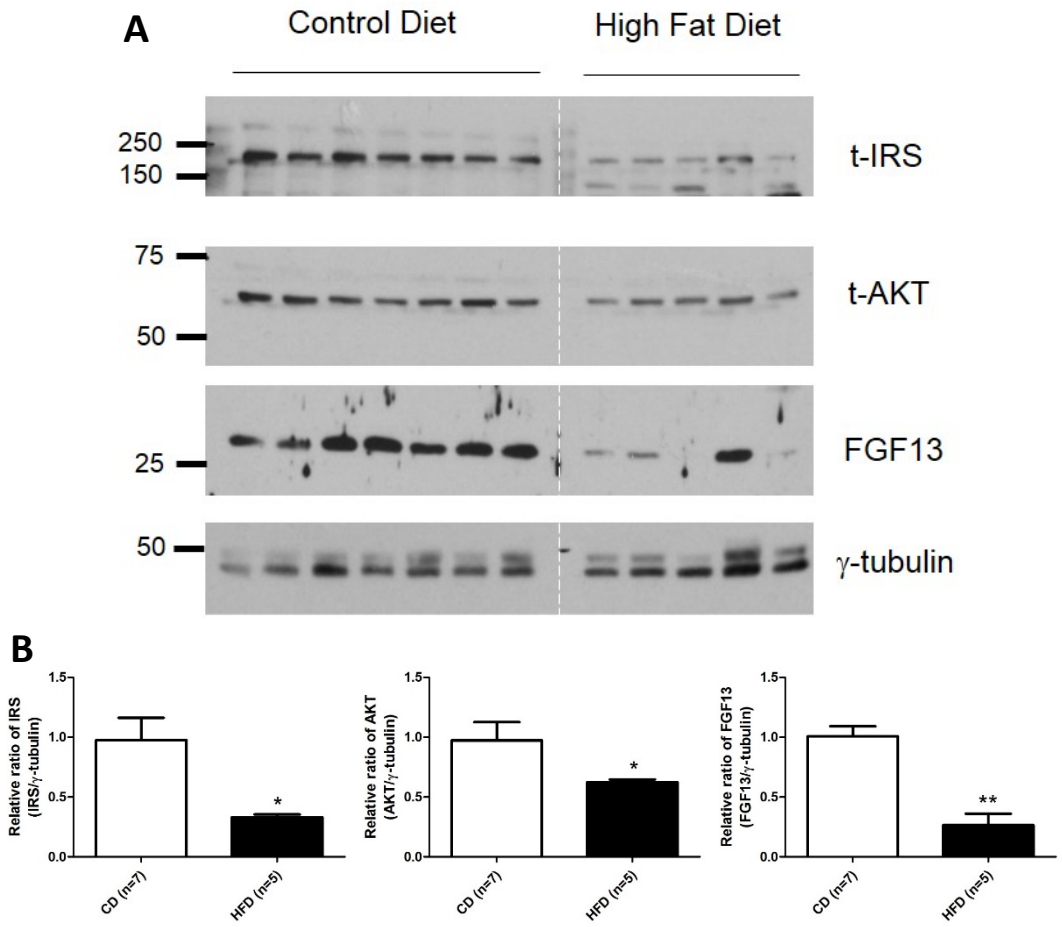

Figure 5. FGF13 protein expression is reduced in white adipose tissue from rodent model of insulin resistance.

(A) Male B6 mice were fed with control diet (CD, n=7) or with high fat diet (HFD, n=5) for 12 weeks, and then sacrificed. White adipose tissues were immunobloted to detect IRS, AKT and FGF13 protein expression. (B) IRS, AKT and FGF13 protein level normalized by γ-tubulin (*$p<0.05$, **$p<0.005$ vs CD).

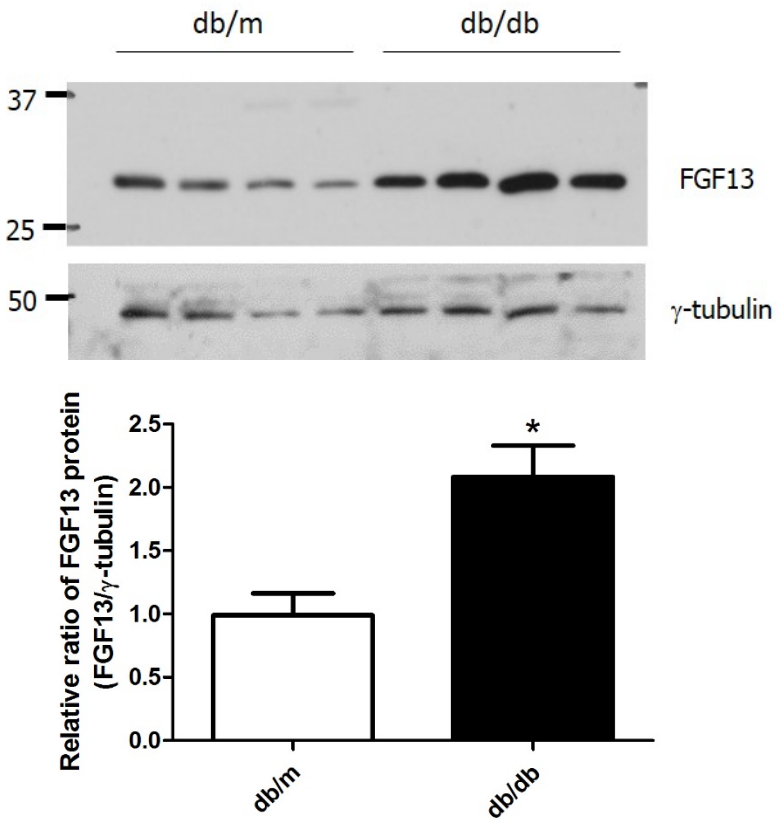

Figure 6. Expression of FGF13 in white adipose tissue of db/db mouse

FGF13 protein expression is increased in white adipose tissue of obese diabetic db/db mice compared with control db/m mice. (*p<0.05 vs db/m)

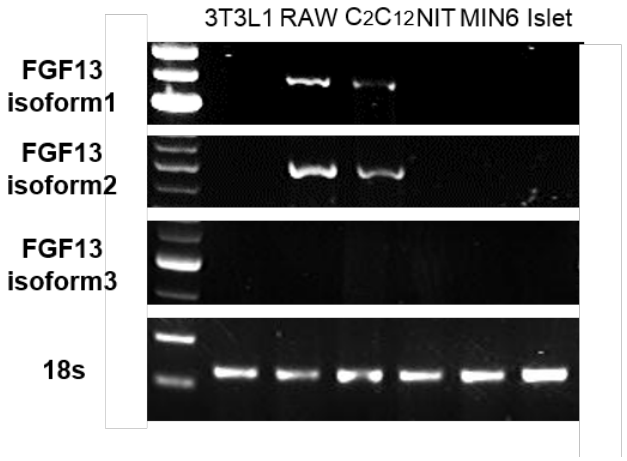

Figure 7. RNA Expression of FGF13 isoform 1, 2 and 3 in mouse cell lines

mRNA of mouse tissue was subjected to RT-PCR for 25 cycles with primers designed for specific FGF13 isoforms (listed on table 1). The housekeeping gene 18s was amplified for 15 cycles.

III. Factors regulating FGF13 expression in cultured skeletal muscle cell

Obesity linked mediators alters FGF13 gene expression

To examine possible regulating factors associated with decreased FGF13 in DIO mice, expression of FGF13 was measured under incubation of 500 μM palmitate, 100 μM oleate, 100 nM TNFα, 100 nM IL6, 3 μM rotenone or 10 μM oligomycin in C2C12 cells for 24 hours. Out of all factors, palmitate and oligomycin showed significant decrease of FGF13 expression (Fig. 8).

Palmitate-induced decreases FGF13 gene expression

To further analyze whether palmitate induces decrease of FGF13 in dose and time dependent manner, protein expression of FGF13 was observed in C2C12 myotubes incubated with 100 μM, 300 μM or 500 μM palmitate for 24 or 48 hours. Decrease of FGF13 was apparently induced by dose and time effect of palmitate treatment. IL6 mRNA increased dose and time dependently with palmitate treatment (Fig. 9).

siTLR4 transfection reverses the effect of palmitate on FGF13 expression

Toll like receptor 4 (TLR4) was knockdown on day 3 of C2C12 differentiation to inhibit its effect on palmitate. As expected, expression of FGF13 was not decreased by palmitate in absence of TLR4. Figure 10 shows that palmitate-induced FGF13 reduction is mediated by TLR4.

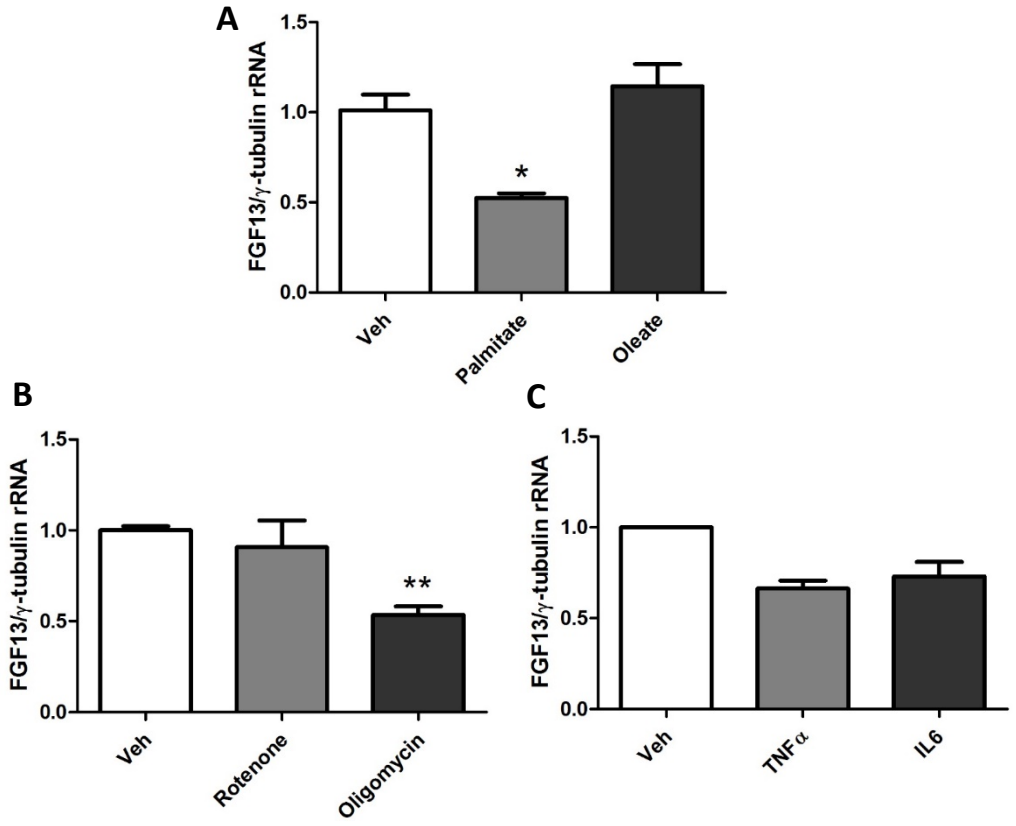

Figure 8. Effect of different fatty acids and inflammatory factors on FGF13 expression

mRNA expression of FGF13 was assessed in C2C12 myotubes incubated with (A) 500 µM palmitate, 100 µM oleate, (B) 3 µM rotenone and 20 µM oligomycin (C) 100 nM TNFα, IL6 (*p<0.05, **p<0.005 vs relative vehicle)

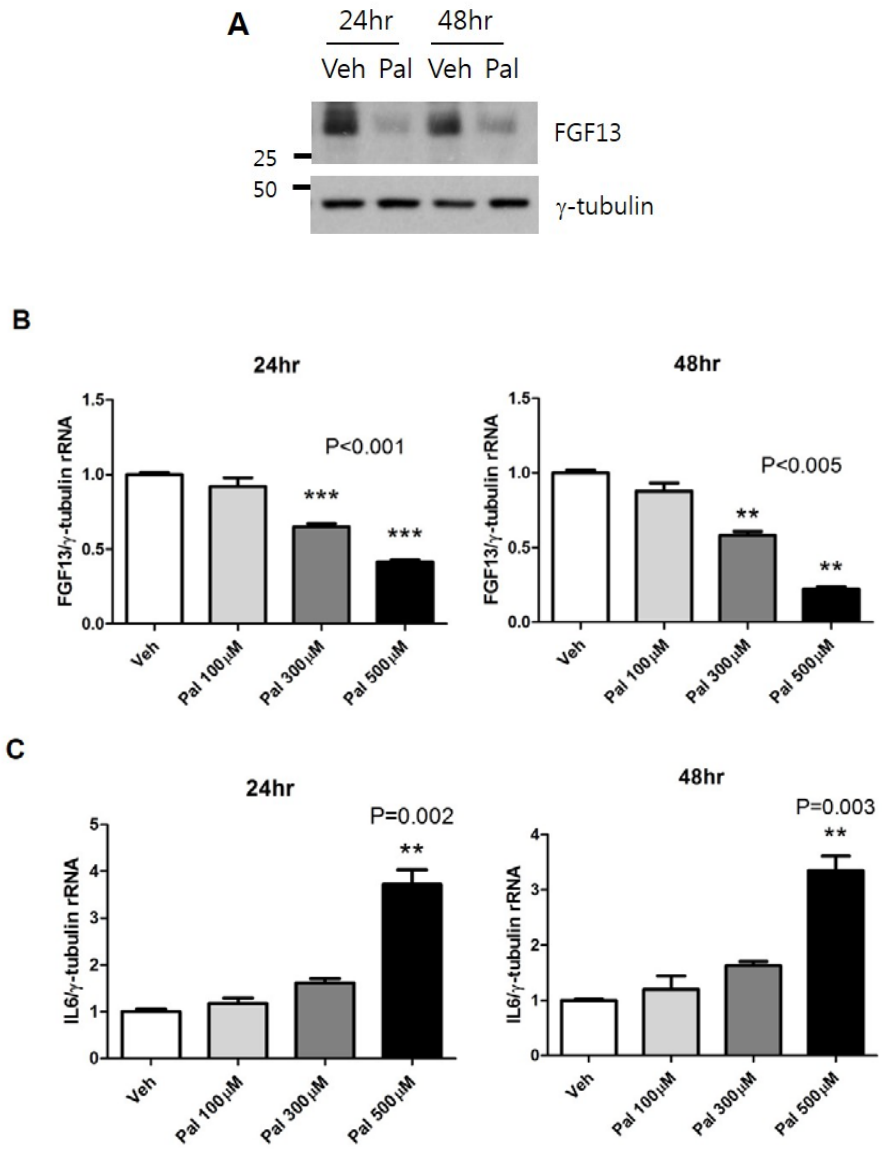

Figure 9. Palmitate decreases expression of FGF13 in C2C12 in time and dose dependent manner.

(A) Representative blot of FGF13. Protein level of FGF13 is decreased by 500 μM palmitate treatment for 24 hours and 48hours. (B) Relative mRNA expression of FGF13 with palmitate treatment in C2C12 cell with palmitate incubation of 100 μM, 300 μM, 500 μM at 24 hours or 48 hours.

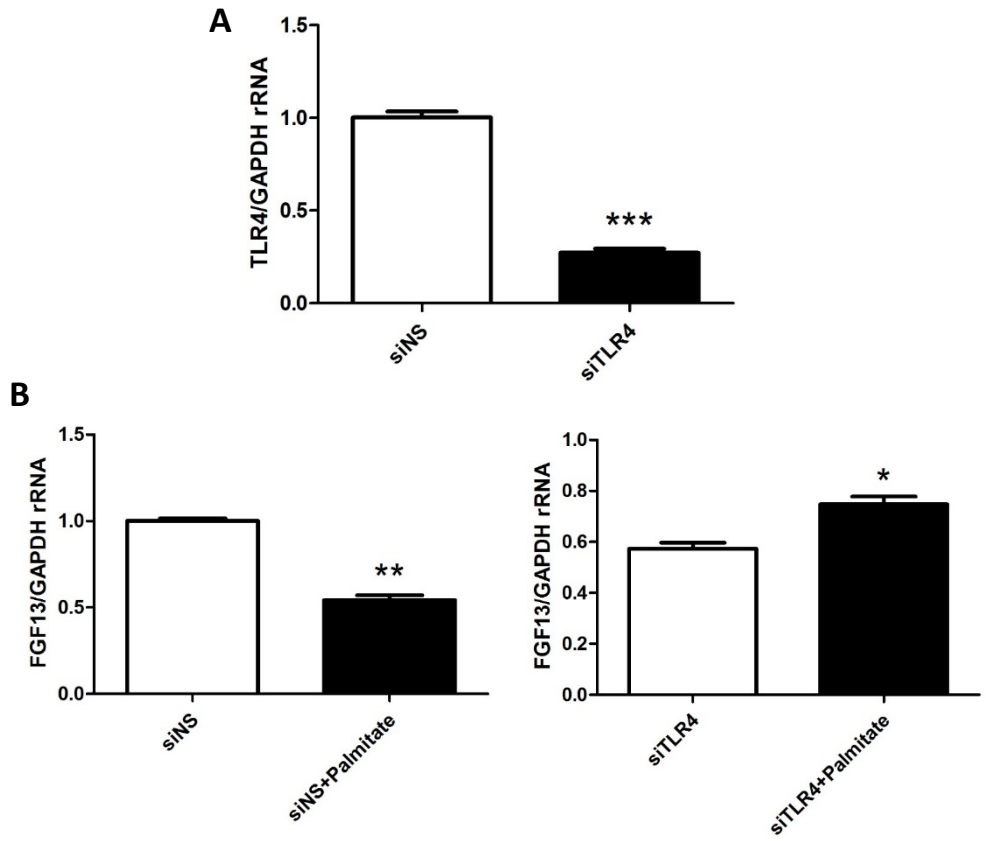

Figure 10 Knockdown of TLR4 reverses the effect of palmitate on FGF13 expression

(A) Relative TLR4 expression in C2C12 myotubes on siTLR4 transfection on day 3 showing 73 % reduction compare to siNS (B) Relative mRNA expression of FGF13 in C2C12 myotubes treated with 500 µM palmitate for 24 hours with siNS or siTLR4 transfection (*$p<0.05$, **$p<0.005$, ***$p<0.001$ vs relative control)

IV. Functional role of FGF13 on MAPK

siFGF13 decreases mRNA expression of immediate early genes.

To examine whether knockdown of FGF13 affects immediate early genes in C2C12 cells, 100 nM of siFGF13 was transfected in C2C12 cell. With 100 nM transfection of siFGF13, C-Fos, C-Jun and EGR1 were all decreased by 50% (Fig. 11).

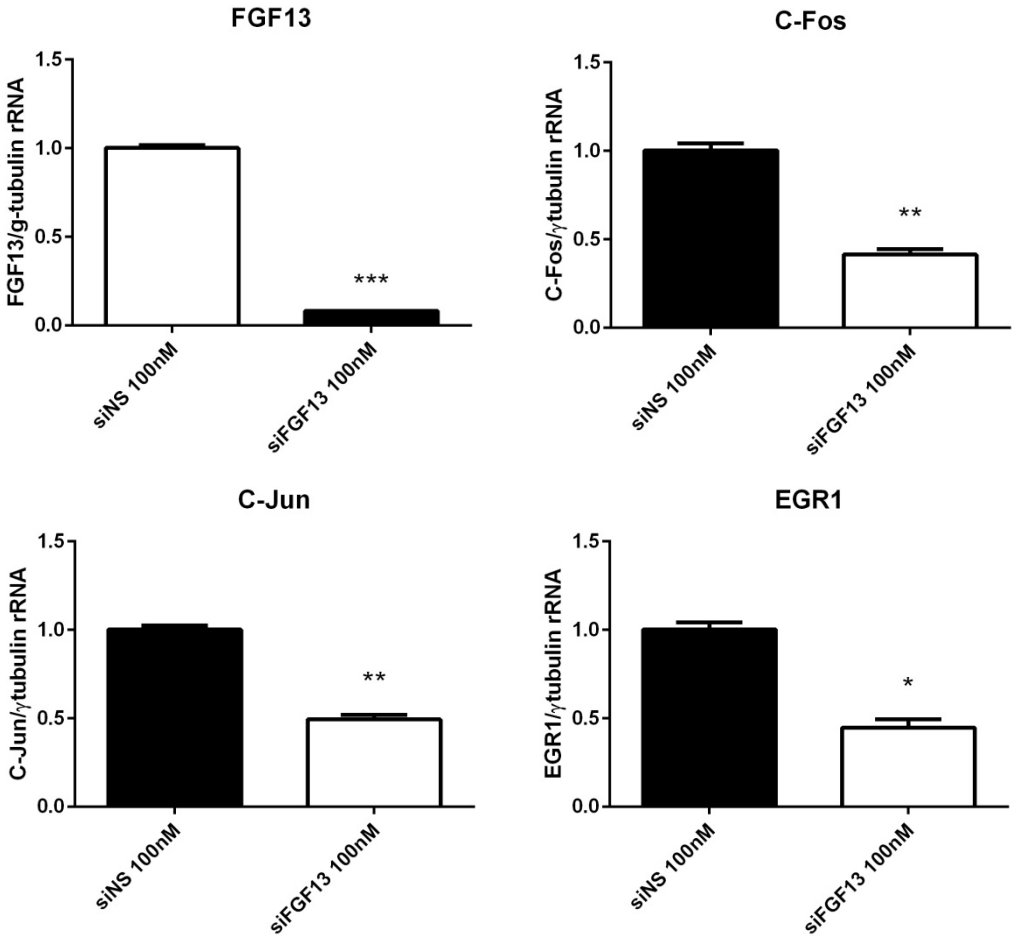

Figure 11. Knockdown of FGF13 decreased in EGR1, C-Fos and C-JUN mRNA level

siFGF13 transfection in C2C12 showed significant reduction in C2C12 cells. Relative mRNA level of EGR1, C-Fos, and C-Jun was decreased by 100 nM of siFGF13 transfection100 nM (*$p<0.05$, **$p<0.005$, ***$p<0.001$ vs siNS).

V. Functional role of FGF13 in insulin signaling pathway

Effect of FGF13 overexpression on insulin and MAPK signaling proteins

Adeno-FGF13 was constructed to overexpress in C2C12 myotubes. In figure 12, palmitate was treated at 500 μM for 24 hours and insulin was given for 15 minutes prior to cell harvest. Under palmitate treatment, I was able to confirm decrease of IRS and AKT signaling and increase of JNK phosphorylation. Overexpression of ad-FGF13 did not show recovery of IRS phosphorylation compared to control ad-GFP in palmitate induced insulin resistance. However, phospho AKT form was recovered by overexpression of FGF13. Moreover, phosphorylation of JNK was remarkably inhibited by overexpression of FGF13.

Effect of FGF13 knockdown on insulin and MAPK signaling proteins

siFGF13 was transfected on day 3 of C2C12 differentiation. Compare to the overexpression study, when FGF13 was knockdown, phosphorylation of AKT was reduced while phosphorylation of JNK was increased (Fig.13). This is very preliminary experiment that needs more of repetitive experiment.

Knockdown of FGF13 reduces mRNA expression of PGC1a and GLUT4

Moreover, under FGF13 knockdown in C2C12, expression of PGC1a and GLUT4 was decreased by half fold (Fig 14). This result indicates that FGF13 may have functional role in mitochondrial biogenesis or glucose transport.

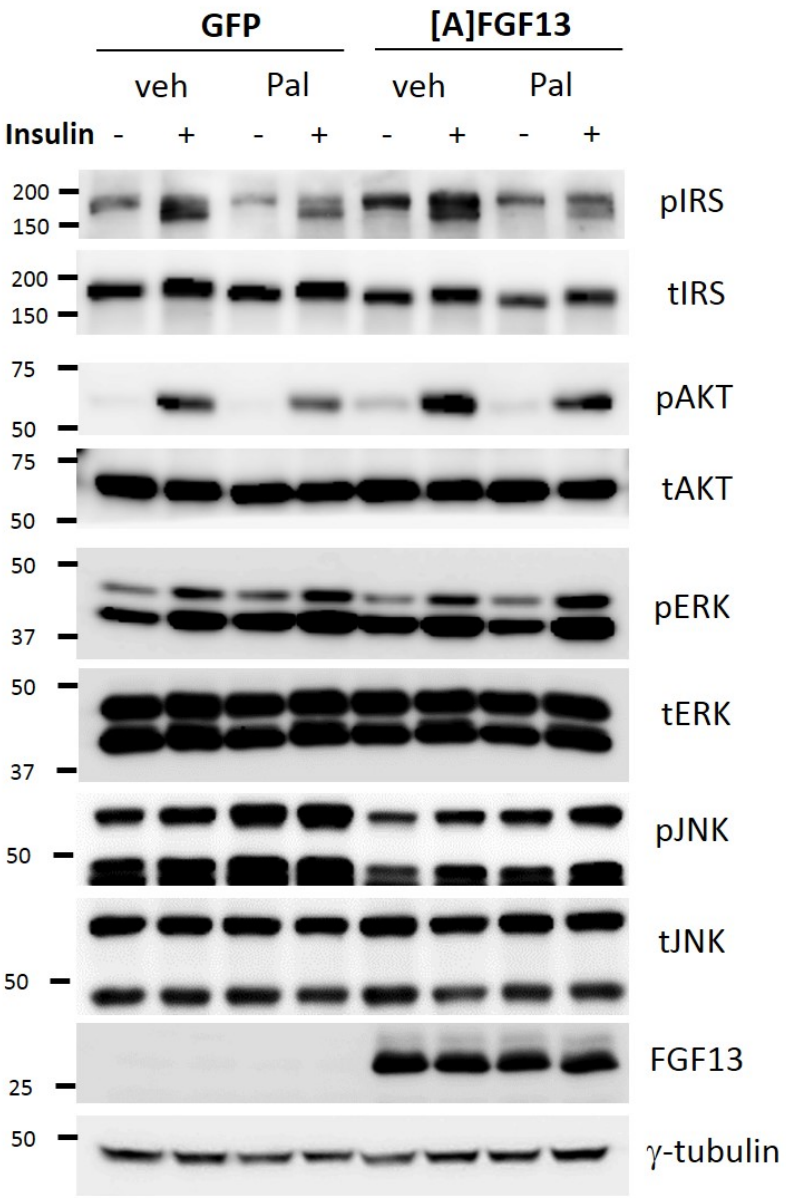

Figure 12. Effect of FGF13 overexpression on insulin and MAPK signaling proteins.

Ad-GFP and ad-FGF13 was infected by 50 moi on day 3 of C2C12 differentiation. Palmitate was given for 24 hours at 500 μM and insulin was induced 15 minutes prior to cell harvest on day 6.

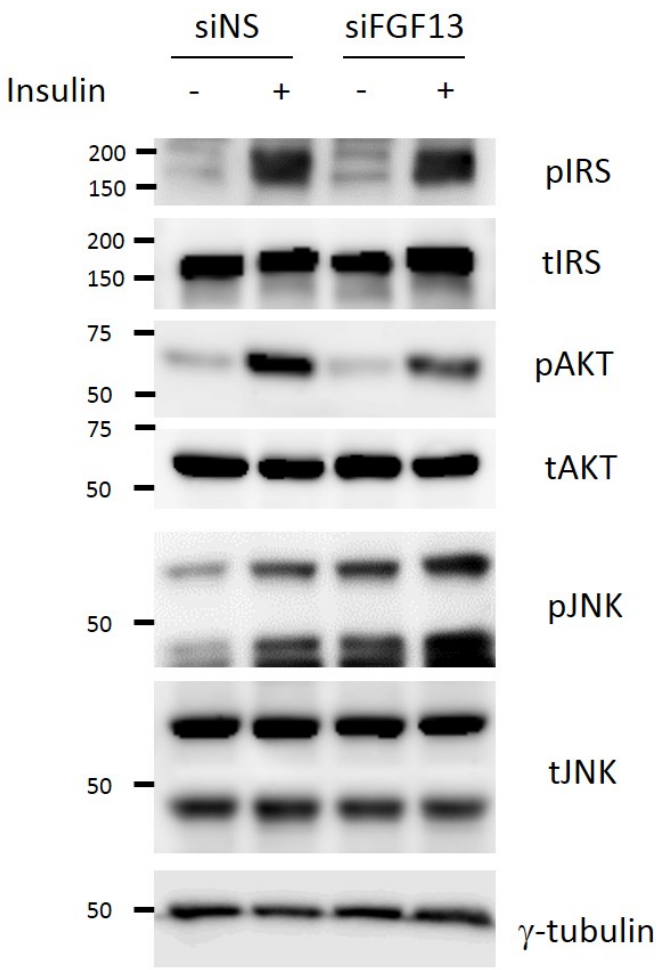

Figure 13. Effect of FGF13 knockdown on insulin and MAPK signaling proteins

siFGF13 was transfected on day 3 of C2C12 differentiation and cells were harvested on day 6. Insulin was induced 15 minutes prior to cell harvest.

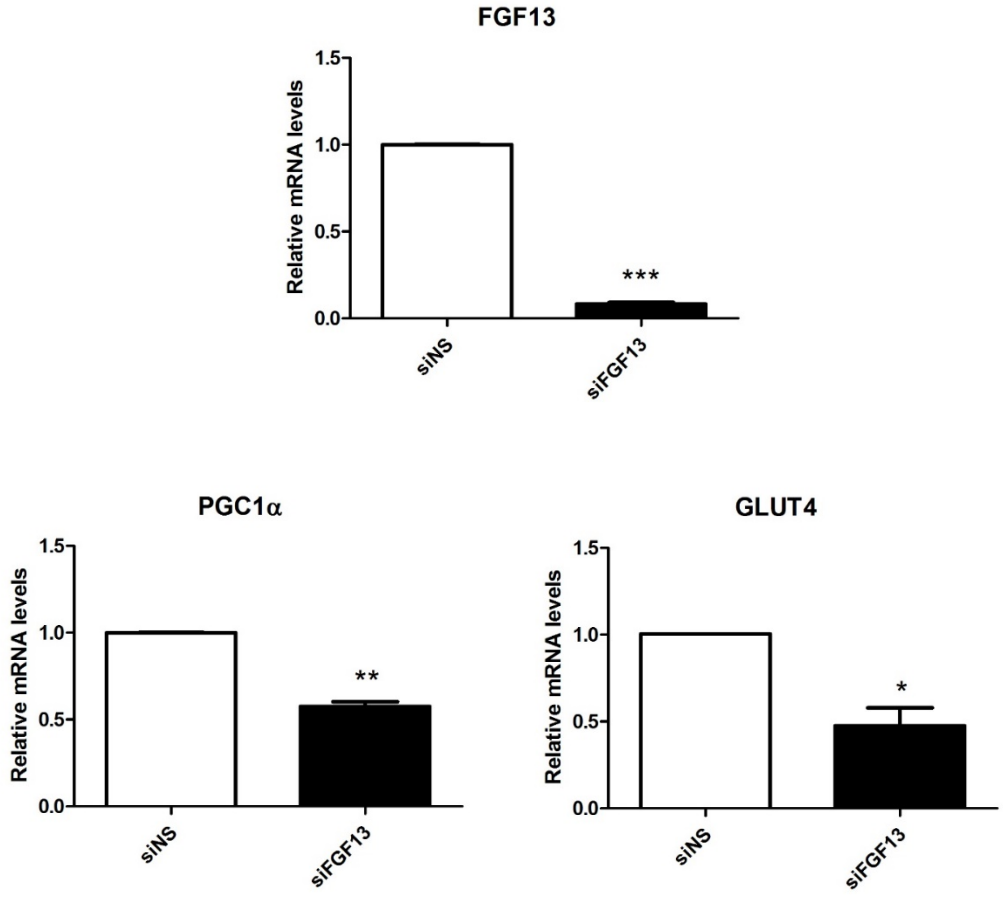

Figure 14. Knockdown of FGF13 reduces mRNA expression of PGC1α and GLUT4

FGF13 was knockdown on day 3 of C2C12 differentiation and relative mRNA levels of PGC1α and GLUT4 were measured. mRNA expression of PGC1α and GLUT4 decreased by knockdown of FGF13. (*$p<0.05$, **$p<0.005$, ***$p<0.001$ vs siNS).

Discussion

In this study, I found that FGF13 isoform showed distinct expression in tissue specific manner. FGF13 isoform 1 was mainly expressed in brain and adipose tissues while isoform 2 was in heart and skeletal muscle. Isoform 3 was expressed in adipose tissues only. Expression of FGF13 was significantly reduced in white adipose tissue and skeletal muscle of DIO mice. Among various potential factors contributing to insulin resistance in obesity, palmitate significantly decreased the expression of FGF13 via TLR4 pathway in C2C12 skeletal muscle cells. Interestingly FGF13 affected AKT and JNK phosphorylation in muscle cells. Taken these data together, FGF13 may play a role in metabolic regulation in skeletal muscle cell.

Intracellular FGFs are known to take a role in transcription regulation signaling and a study demonstrated that FGF13 interacts with mitogen-activated protein kinase 8 interacting protein 2 (MAPK8IP2) which is the JNK-interacting protein (JIP) group of scaffold proteins [6]. FGF13 was knockdown to measure mRNA level of immediate early genes in MAPK pathways. These genes include c-Fos, c-Jun and EGR1 and they were all decreased by half fold when FGF13 was knockdown. This result suggests that FGF13 may affect MAPK pathway in skeletal muscle cells.

As shown in figure 12, FGF13 overexpression did not alter or recover palmitate induced decrease in tyrosin phosphorylation of IRS. However, FGF13 overexpression restored AKT phosphorylation which was decreased with palmitate treatment. In line with FGF13 overexpression, FGF13 knockdown showed opposite effect on AKT phosphorylation. Interestingly, FGF13 overexpression significantly reduced JNK signal in palmitate treated C2C12 cells. This result is very intriguing since free fatty acid interrupts insulin signaling by activating the JNK signal [14]. More experiments need to be done to see how FGF13 takes role in this pathway.

Moreover, knockdown of FGF13 decreased levels of peroxisome proliferator-activated receptor c coactivator 1α (PGC1α) and glucose transporter type 4 (GLUT4) (Fig 14). PGC1α is a inducer for mitochondrial biogenesis of the cell and GLUT4 is mainly responsible for insulin stimulated glucose transport [15, 16]. Further study needs to be done to find out whether FGF13 takes a role in mitochondrial biogenesis or glucose transport in skeletal muscle cell.

This study had several limitations. FGF13 was significantly reduced in DIO while it was highly expressed in db/db mouse model. These different expression pattern of FGF13 in two different mouse model of obesity indicates that FGF13 expression may be affected by genetic complexities in

diabetic db/db mice such as defective leptin signaling. Moreover, even though FGF13 certainly showed high expression in mouse white adipose tissue, I could not detect FGF13 isoforms in 3T3L1 adipocytes.

Overall, this study demonstrates that FGF13 is decreased in DIO model and reduced by palmitate acid in skeletal muscle. Also, I observed that knockdown of FGF13 decreases immediate early genes in MAPK pathway (c-Jun, c-Fos, EGR1) which indicates that FGF13 may play role with MAPK in skeletal muscle cell. However, exact mechanism of FGF13 on insulin action and metabolism in skeletal muscle remains largely unknown. Therefore, this tissue-specific models of FGF13 isoform 2 in mice will be required to understand the essential effect of FGF13 on skeletal muscle.

Conclusion

FGF13 has three major isoforms which are distinctively expressed in various tissues. FGF13 isoform 1 is specifically distributed in brain and adipocytes while FGF13 isforom 2 showed expression in heart and skeletal muscle only. On the contrary, expression of FGF13 isoform 2 could be detected in C2C12 myotubes and macrophage RAW cells. Saturated fatty acid mediates decreased expression of FGF13 isoform 2. This effect appear to be meditated by TLR4 pathway. Furthermore, RNA level of immediate early genes of MAPK was reduced by knockdown of FGF13 in C2C12. When FGF13 was overexpressed, it recovered AKT signal under palmitate induced insulin resistance. On the contrary, it reduced JNK signal activated by palmitate. These findings suggests that FGF13 may play role in metabolic pathway.

References

1. Itoh, N. and D.M. Ornitz, *Fibroblast growth factors: from molecular evolution to roles in development, metabolism and disease.* J Biochem, 2011. **149**(2): p. 121-30.
2. Ornitz, D.M. and N. Itoh, *Fibroblast growth factors.* Genome Biol, 2001. **2**(3): p. reviews3005.
3. Woo, Y. C., et al, *Fibroblast Growth Factor 21 as an emerging metabolic regulator: clinical perspectives*. Clin Endocrinol , 2013. **78**, p. 489–496.
4. Muise, E., et al, *Adipose Fibroblast Growth Factor 21 Is Up-Regulated by Peroxisome Proliferator-Activated Receptor γ and Altered Metabolic States.* Mol Pharm, 2008. **74**: p. 403–412.
5. Zhang, X., et al., *Receptor specificity of the fibroblast growth factor family. The complete mammalian FGF family.* J Biol Chem, 2006. **281**(23): 15694-700.
6. Schoorlemmer, J. and Goldfarb, M. *Fibroblast Growth Factor Homologous Factors and the Islet Brain-2 Scaffold Protein Regulate Activation of a Stress-activated Protein Kinase.* J. Biol. Chem., 2002. **277**: 49111-49119.

7. Olsen, S.K., et al., *Fibroblast growth factor (FGF) homologous factors share structural but not functional homology with FGFs.* J Biol Chem, 2003. **278**(36): p. 34226-36.

8. Gecz, J., et al., *Fibroblast growth factor homologous factor 2 (FHF2): gene structure, expression and mapping to the Borjeson-Forssman-Lehmann syndrome region in Xq26 delineated by a duplication breakpoint in a BFLS-like patient.* Hum Genet, 1999. **104**(1): p. 56-63.

9. Wu, Q.F., et al., *Fibroblast growth factor 13 is a microtubule-stabilizing protein regulating neuronal polarization and migration.* Cell, 2012. **149**(7): p. 1549-64.

10. Cheng, A. and Fantus G., *Oral antihyperglycemic therapy for type 2 diabetes mellitus*. CMAJ 2005. **172**(2):213-26

11. Taube, A. et al., *Role of lipid-derived mediators in skeletal muscle insulin resistance.* Am J Physiol Endocrinol Metab, 2009. **297**: E1004–E1012.

12. Boden, G., *Obesity and free fatty acids.* Endocrinol Metab Clin North Am, 2008. **37**(3): p. 635-46, viii-ix.

13. Yu C, Chen Y, Cline GW, et al. *Mechanism by which fatty acids inhibit activation of insulin receptor substrate-1 (IRS-1)-associated phosphatidylinositol 3-kinase activity in muscle.* J Biol Chem 2002. **277**: p. 50230–50236.

14. Saltiel A. and Kahn C., *Insulin signaling and the regulation of glucose and lipid metabolism*. Nature 2001. **414**: p. 799–806.

15. Finck B. and Kelly D., *PGC-1 coactivators: inducible regulators of energy metabolism in health and disease*. J. Clin. Invest. 2006. **116**: p. 615–622.

16. Huang S. and Czech M., *The GLUT4 Glucose Transporter*. Cell Metab 2007. **5**: p.237-52

국문 초록

제 2 형 당뇨병 환자에서 가장 먼저 발견되는 현상은 인슐린 저항성과 골격근에서 지방의 축척이다. Free fatty acid 가 비만과 당뇨병에 미치는 메커니즘이 다양하게 적용되는 가운데 보통 포화지방산이 IRS, AKT, PI3K 등 인슐린 기능을 컨트롤 하는 유전자에 영향을 끼친다고 알려져 있다. 본 연구에서는 free fatty acid 가 어떤 기전으로 Fibroblast Growth Factor 13 (FGF13) 발현을 변화시키는지에 대해 알아보았다.

FGF13 은 Fibroblast Growth Factor 군의 일원으로써 미세 소관 안정화와 신경세포 편광에 중요한 역할을 한다고 알려져 있다. 이 유전자는 다양한 신경학 연구에서 관찰되어있지만 아직 대사질환분야에서는 연구가 되어지지 않았다. 본 연구의 목적은 다양한 FGF13 isoform 의 유전자 발현과 기능을 알아보고자 하였다. 12 주간 고지방 다이어트를 한 쥐와 일반식을 먹인 쥐의 지방과 골격근에서 FGF13 isoform 들의 RNA 발현양을 비교해 보았다. 그 결과 FGF13 isoform 1 은 주로 지방 조직에 발현 되어있었고 isoform 2 는 주로 골격근에 발현을 하였다. 또한 고지방 다이어트를 한 쥐에서 FGF13 isoform 1, 2 모두 감소한 결과를 얻을 수 있었다.

따라서 주로 비만과 당뇨병 중재자 역할을 하는 포화지방산과 염증인자를 생쥐 골격근 세포주인 C2C12 myotube 에 처리하여 어떤 기전으로 발현 양이 감소하는지 알아보았다. 그 결과 동물실험결과와 동일하게 palmitate, TNFα 그리고 oligomycin 등에 의하여 FGF13 발현 양이 감소하였다. Palmitate 를 노출시키는 시간과 양에 비례하여 FGF13 이 더욱더 감소하는 경향을 볼 수 있었고 이는 TLR4 pathway 를 통함을 확인하였다. 또한, FGF13 이 insulin signaling 에 관련이 있는지 알아보기 위해 FGF13 Adeno-virus 를 C2C12 myotube 에 과 발현 시킨 palmitate 에 의하여 감소된 AKT signaling 을 회복시킴을 확인하였다. 흥미롭게도, FGF13 을 과 발현시켰을 때 palmitate 에 의하여 증가되는 JNK 인산화가 억제되는 결과도 확인할 수 있었다.

이 연구들을 통하여 FGF13 이 대사질환에서 어떻게 작용하는지 처음으로 규명되었다. 비록, FGF13 이 인슐린 저항성을 조절하는 기전에 있어서 추가적인 연구가 필요하지만 FGF13 이 AKT 와 JNK 인산화를 조절하며 인슐린조절을 위한 표적 단백질이 될 수 있을 것이라 할 수 있다.

주요단어: Fibroblast Growth Factor 13, 인슐린 저항성, 지방산, 비만 당뇨
학번: 2013-24045